Clim. Past Discuss., 7, 1427–1455, 2011
www.clim-past-discuss.net/7/1427/2011/
doi:10.5194/cpd-7-1427-2011

Climate of the Past Discussions

Precessional and half-precessional climate forcing of Mid-Devonian monsoon-like dynamics

D. De Vleeschouwer[1], A. C. da Silva[2], F. Boulvain[2], M. Crucifix[3], and Ph. Claeys[1]

[1]Earth System Sciences, Vrije Universiteit Brussel, 1050 Brussels, Belgium
[2]Pétrologie sédimentaire, B20, Université de Liège, Sart Tilman, 4000 Liège, Belgium
[3]Centre de recherche sur la Terre et le climat Georges Lemaître, Earth and Life Institute, Université catholique de Louvain, 1348 Louvain-la-Neuve, Belgium

Received: 2 April 2011 – Accepted: 21 April 2011 – Published: 2 May 2011

Correspondence to: Ph. Claeys (phclaeys@vub.ac.be)

Published by Copernicus Publications on behalf of the European Geosciences Union.

Abstract

A Devonian magnetic susceptibility (MS) record obtained on limestones ranging from the Uppermost-Eifelian to the Lower-Givetian and located on the southern border of the Dinant Synclinorium in Belgium, was selected for time-series analysis. In these carbonate ramp and platform deposits, spectral analyses highlight persistent high-frequency cycles in both the MS-signal and the microfacies curve, reflecting environmental and climate changes. These meter-scale variations in the MS-signal are interpreted as changes in the flux of magnetic minerals towards the marine system, most likely controlled by monsoon rainfall-intensity. By combining chrono- and biostratigraphic information with theoretical knowledge of sedimentation rates in different depositional environments, these cycles are interpreted as astronomically driven (precession-dominated). It is hypothesized that during precession maxima the trans-equatorial pressure gradient reaches a maximum and intensifies monsoonal circulation. The consequent increased moisture transport towards the continent leads to enhanced precipitation and runoff, which in turn leads to an increased flux of detrital material (including magnetic minerals responsible for the MS-signal) towards the marine system. Moreover, this unique high-resolution climate signal reveals half-precessional cycles. These cycles suggest the important response of intense monsoonal systems to periodic changes in the strength of low-latitude (equatorial) insolation.

1 Introduction

It is only since the late seventies that variations in the Earth's orbit were accepted as the pacemaker of the Quaternary ice ages (Hays et al., 1976). To leave the sphere of controversy, the theory needed several well-established feedback mechanisms and assumptions about the nonlinear responses of ice sheets to the applied astronomical forcings. In an extreme hot, greenhouse world, without any major ice sheets, ice-related feedback mechanisms and nonlinearities do not longer apply. Consequently,

CPD
7, 1427–1455, 2011

other mechanisms must explain the amplification of subtle variations in the Earth's orbital parameters into global climate and environmental changes. Except for the important positive water vapor feedback mechanisms (Rind et al., 1991; Flohn et al., 1992) and the vegetation and soil feedback mechanism (Kutzbach et al., 1996; Dekker et al., 2007), a clear understanding of how this amplification occurred in an ice-free hot greenhouse world is lacking.

The Greenhouse Devonian Period (418–361 Ma, Kaufmann, 2006) is characterized by climate boundary conditions that are completely different compared to the Quaternary: atmospheric CO_2 concentration was up to 10 times higher compared to today's value (Berner, 2006), continents were concentrated in the Southern Hemisphere (SH), global temperatures and sealevels were high and vast shallow epicontinental seas allowed reefs to develop at unusually high latitudes, reaching 65° N–55° S during the Middle-Devonian (Copper, 2002). Moreover, the Devonian is a key-period in the evolution of life on Earth. E.g., the fish-tetrapod transition occurred during the early Middle-Devonian (Niedzwiedzki et al., 2010). In this study, we applied the mathematical techniques of time-series analyses on a well-known 85m-thick Eifelian/Givetian (Middle-Devonian) section from Southern Belgium (Mabille and Boulvain, 2007; Boulvain et al., 2010). The studied section, characterized by a high accumulation rate and high sampling resolution, comprises a climate signal that is highly suitable to study the influence of Milanković (eccentricity, obliquity and precession) and sub-Milanković cycles on the Middle-Devonian climate of the Rhenohercynian Basin. The main objective of this study is to reveal the finger print of these cycles in the section, so to obtain a better insight into the response of an extremely hot Greenhouse climate to astronomical forcing.

2 Geological setting

The Eifelian-Givetian "La Couvinoise" quarry is located along the southern flank of the Dinant Synclinorium, in Southern Belgium, which is part of the Rhenohercynian

CPD
7, 1427–1455, 2011

fold-and-thrust belt (Fig. 1). The studied section corresponds to a mixed carbonate-siliciclastic ramp. It has been subdivided in different microfacies corresponding to two main depositional settings: open-marine at the base of the section and fore-reef at the top (Fig. 2; Mabille and Boulvain, 2007). Open-marine facies correspond to a succession of argillaceous mudstones to carbonates composed of packstones with crinoids and brachiopods. Rudstones with stromatoporoids debris, tabulate and rugose corals, followed by packstones and grainstones with peloids characterize the overlying fore-reef carbonate facies (Mabille and Boulvain, 2007).

3 Materials and methods

3.1 Magnetic susceptibility

Magnetic susceptibility (MS) represents the degree of magnetization of a material in response to an applied magnetic field. It quantitatively measures the amount of magnetic minerals in a sample. The MS of a sediment forms a proxy for the rate of supply of the magnetic susceptible lithogenic or detrital fraction to the marine system (Ellwood et al., 2000). In the studied section, large-scale MS variations can be ascribed to relative sea-level changes (Mabille and Boulvain, 2007; da Silva et al., 2009). On a shorter time-scale, climate, through the intensity of wind and precipitation, plays a decisive role in determining respectively the eolian and riverine flux of magnetic minerals to the marine system (Hladil et al., 2006; Riquier et al., 2010) as it was in this case the Rheic Ocean (Fig. 1). In today's world, the response of different tropical monsoon systems to orbital, Milanković forcing is clearly demonstrated (e.g., Kutzbach, 1981; Kutzbach and Liu, 1997; Tuenter et al., 2003). Compared to today, the Devonian tropical climate potentially exhibited an even more intense monsoonal circulation (Streel et al., 2000), characterized by seasonally wet-and-dry climates (Cecil, 1990). Consequently, it is highly probable that also during the Devonian period, Milanković cycles influenced the

CPD
7, 1427–1455, 2011

climatic factors controlling the detrital inputs to the basins (i.e. wind and precipitation) and/or of carbonate productivity, both affecting the MS signal (Riquier et al., 2010).

3.2 Time-series analysis procedure

The frequency composition of the magnetic susceptibility signal is analyzed via spectral analysis, using the multitaper method (MTM; Thomson, 1982), as implemented in the SSA-MTM Toolkit (Ghil et al., 2002). Before the implementation of MTM spectral analysis, long-term trends were removed from the MS data by subtracting the continuous linear trend. The MTM-method was performed using 3 tapers to compromise between resolution and sidelobe reduction. Trading resolution for sidelobe reduction is needed because small variations in accumulation rate behave like phase modulations, and introduce erroneous spectral peaks (Muller and MacDonald, 2000). The MTM averages these sidelobes into the main peak and thereby provides a better estimate of the true spectral power. Noise in paleoclimate signals is frequently "1/f noise" or "red noise", which means that the power spectrum of the background shows a strong enhancement at the low frequency end (Muller and MacDonald, 2000). The 90 % and 99 % confidence limits (CLs) are calculated to visualize the most significant deviations from the null hypothesis of red noise.

The microfacies curve is obtained by digitizing the microfacies log, resulting in square wave data. The step-like changes in microfacies can only be represented using multiple additional sine and cosine components during a Fourier transformation, polluting the spectrum (Proakis and Menolakis, 1996; Weedon, 2003). Therefore, spectral analysis on the microfacies curve was carried out using the Walsh and Blackman-Tukey (BT) method for spectral analysis. Walsh power spectra are based on the use of square waves instead of sine and cosine waves. The equivalent of a Fourier Transform can be generated using the Walsh transform (Beauchamp, 1975; Weedon, 1989). The Blackman-Tukey method is based on the Fourier transform of part of the autocovariance sequence. The autocovariance sequence contains the same frequency oscillations as the microfacies series, but is no longer characterized by step-like changes.

CPD
7, 1427–1455, 2011

Frequency-selective filters or band-pass filters are able to isolate a specific range of frequencies from a signal. Consequently, it is an excellent device to assess the behavior of a specific range of frequencies in a studied signal. We used the Analyseries software to calculate the filtered signals (Paillard et al., 1996).

The analysis of amplitude modulations (AM) constitutes a useful tool in cyclostratigraphy: The astronomical theory states that the amplitude of the precession parameter is modulated by eccentricity. To examine possible amplitude modulations in the studied signal, the precession parameter was first extracted from the signal by band-pass filtering. Subsequently, its amplitude envelope was extracted by complex demodulation, based on the Hilbert transform (Bloomfield, 2004).

3.3 Possible distortions of the astronomical frequencies

When interpreting cyclic sedimentary alternations as a consequence of periodic changes in the orbital parameters of the Earth, one should be aware of the fact that the assumption of a 1:1 recording of astronomical signals in carbonate sediments is questionable (Westphal et al., 2004). The original astronomical signal can be altered by the climatic system, responding in a nonlinear way to the applied forcing. Moreover, a sediment column recording climatic changes never represents these temporal changes in a linear manner. For example, variations in sedimentation rate, bioturbation, differential compaction and pressure dissolution can be responsible for distortions of the orbital frequencies in sedimentary records. To account for these possible overprinting factors, some assumptions and restrictions must be respected. On carbonate platforms and ramps, sediment production rate is above other factors, a function of carbonate productivity. The main trend is a decrease in the carbonate productivity with increasing depth, with maximum carbonate production in the reefal environments (da Silva et al., 2009). Therefore, the two main sedimentary environments represented in the "La Couvinoise" section (Fig. 2) are characterized by significantly different accumulation rates: it is expected that a significantly higher accumulation rate characterizes the fore-reef environment compared to the open-marine environment (da Silva et al., 2009). In

CPD
7, 1427–1455, 2011

depositional environments with different accumulation rates, cycles of equal duration will be expressed by sediment packages of different thickness. This phenomenon could render the application of spectral analysis on a distance-series including different depositional settings impossible. However, if one assumes that accumulation rate within the same sedimentary environment is semi-constant, MTM-spectral analysis can be carried out for the two main sedimentary environments of the "La Couvinoise" section separately. For the "La Couvinoise" section no indications for hiatuses or for differential compaction within a sedimentary environment are found.

4 Results and discussion

4.1 Recognition and identification of astronomical cycles

For the open-marine environment, the Walsh and BT spectral plots of the microfacies-data are characterized by an elevated spectral power, around frequency 0.7 (Fig. 3a). Moreover, an increased spectral power that extends above the 99 %CL, can be found at the same frequency on the MTM spectral plot of the MS data. However, around frequency 0.55 m^{-1}, the spectral plot of the MS data reveals an important peak (Fig. 3a). This double peak is not visible in the spectral plot of the microfacies-data, where a relatively wide frequency domain is distinguished by an increased spectral power. Despite the relatively large spectral width between the two peaks in the MS-spectral plot (Fig. 3a), the double peak is seen as the result of one and the same forcing factor, since it might be the result of small variations in accumulation rate in the open-marine environment or of an astronomical forcing parameter with multiple frequencies or – most likely – of a combination of both. The reason this double peak is not developed in the microfacies spectral plot lies entirely within the nature of the data. The microfacies series is characterized by a smaller number of meter-scale variations compared to the MS series, which results in a less accurate recognition of cyclic meter-scale variations by spectral analysis.

CPD
7, 1427–1455, 2011

In the fore-reef environment, the Walsh and BT spectral plots of the microfacies-data (Fig. 3b) exhibit three significant spectral peaks around frequency 0.05 m^{-1}, around 0.3 m^{-1} and around 0.65 m^{-1}. Remarkably, the MTM spectral plot of the MS data reveals the exact same pattern (Fig. 3b). This observation indicates that microfacies and MS record the same environmental changes. Therefore, common indications for astronomical forcing are more credible, whereas differences among both proxies call for a critical evaluation of the extent to which astronomical forcing influenced environmental changes.

The only time-constraint available in the studied section is the existing biostratigraphy and more precisely the delineation of the *ensensis* conodont biozone between the bottom of the section and 33.75 m. The *hemiansatus* conodont zone cannot be used as a time-constraint because its top is not reached in the "La Couvinoise" section. According to the recalibrated "biochronometric" time-scale of Kaufmann (2006), the *ensensis* biozone lasted for ~300 kyr. Consequently, an average sedimentation rate of ~11.3 cm kyr^{-1} can be calculated for this biozone. Under such conditions, sedimentary cycles with a thickness between 1.31 and 1.86 m, have been deposited in 11.6 up to 16.4 kyr. Assuming that these meter-scale cycles are all of (nearly) equal duration and caused by astronomical forcing, they are most likely the result of the Devonian precession cycle (with a period around 18 kyr according to Berger et al., 1992). If this interpretation is correct, the biostratigraphically inferred average accumulation rate (~11.3 cm kyr^{-1}) must be revised downwards to ~8.8 cm kyr^{-1}. Taking into account the relationship in sedimentation rate between the open-marine and fore-reef depositional settings, it is expected that sedimentary cycles related to precession are thicker in the fore-reef environment, compared to the open-marine environment (da Silva et al., 2009). Therefore, in the upper part of the section, the 2.9–3.56 m cycles are interpreted as the result of precession. The 1.34–1.69 m cycles in this part of the section have a period that is half the precessional period. If this interpretation is correct, the average sedimentation rate in this part of the section lies around 18 cm kyr^{-1}. The derived sedimentation rates are from the same order of magnitude as the average

CPD
7, 1427–1455, 2011

sedimentation rate that can be calculated for the whole Givetian for the palaeolocation of Southern Belgium (i.e. 10.5 cm kyr^{-1}; Boulvain et al., 2010) or as the estimates of accumulation rate made for a contemporaneous (Mid-Eifelian to basal-Givetian) section in the nearby Eifel region (Rhenish Massif): 12.53 cm ka^{-1} (Weddige, 1977; Bultynck et al., 1988; Kaufmann, 2006).

The interpretation of the 1.31–1.86 m cycles and 2.9–3.56 m cycles as the result of precessional forcing, in the lower and upper part of the section respectively, renders possible the transformation of the magnetic susceptibility distance-series into a time-series (Fig. 4). The precessional cycles are extracted from the distance-series by band-pass filtering the lower part of the section between frequencies 0.53 and 0.76 m^{-1} (1.31–1.86 m periodicity) and by filtering the upper part of the section between frequencies 0.28 and 0.35 m^{-1} (2.9–3.56 m periodicity; Fig. 4a). By counting the precessional cycles and multiplying them by the period of precession (i.e. ∼18 kyr), the MS-series can be rescaled relative to a time-axis (Fig. 4b). On Fig. 4, 39.3 precessional cycles can be counted in the "La Couvinoise" section. This implies that the section was deposited in ∼710 kyr. When the constructed time-series is band-pass filtered at the frequency of precession (between 0.043 and 0.067 kyr^{-1}, i.e. 15–23 kyr periodicity), a ∼100-kyr cyclicity is observed in the amplitude envelope of the precessional cycles. This observation strongly suggests the amplitude modulation of the precessional cycles by eccentricity (Figs. 4b and 5a).

Using the constructed time-series (Fig. 4b) instead of the distance-series, spectral analysis is again carried out on the MS data (Fig. 5b). The reenactment of spectral analysis brings two significant improvements: First, the "La Couvinoise" section is considered as a whole, rather than in two different parts, so that the continuity of the cycles can be better tested. Second, the problem of accumulation rate variations within a depositional environment is bypassed. The resulting spectral plot (Fig. 5b) shows a very strong peak at the frequency of precession. Of course, the magnitude of this spectral peak is partly conditioned by the procedure of time-axis composition. However, there is no reason to doubt the statistical significance of this peak as the time-axis composition

CPD
7, 1427–1455, 2011

is based on a robust spectral analysis of the MS signals of the different sedimentary environments (Fig. 3). One would expect a spectral peak around 0.03 and 0.01 kyr^{-1} if respectively obliquity and 100-kyr eccentricity would influence the MS signal of the "La Couvinoise" section (Berger et al., 1992). At these frequencies no outstanding spectral peak can be found, advocating that obliquity and eccentricity do not strongly influence the MS signal directly. However, Fig. 5a shows the spectral plot (Fast Fourier Transformation, FFT) of the amplitude envelope of the precession cycles and contains a strong peak around 0.00244 kyr^{-1}, one around 0.00735 kyr^{-1} and one around 0.0108 kyr^{-1} (periodicities 409, 136 and 93 kyr, respectively). These peaks correspond well to the theoretical periods of eccentricity (i.e. 405, 125, 95 kyr). In other words, these results demonstrate that the amplitude envelope of the precession signal is modulated by eccentricity. The recognition of the amplitude modulation of the precession cycles by eccentricity can be considered as an independent confirmation of the accuracy of the time-series construction.

Moreover, on Fig. 5b, another strong spectral peak can be observed around frequency 0.10 kyr^{-1} (9.8 kyr periodicity). This peak seems to suggest the presence of half-precessional cycles recorded in the MS stratigraphy of the "La Couvinoise" section.

In Fig. 6a, the microfacies curve is rescaled and plotted against a time-axis, based on the same procedure as for the MS series. Both the Walsh transform (Fig. 6b) as the Fourier transform (Fig. 6c) were used as the basis for calculating a band-pass filter centered on the frequency of precession (between 15 and 23 kyr). Both filters demonstrate that a large fraction of the microfacies variation in the studied section happens on a precessional time-scale. Moreover, an important amplitude modulation of the precessional signal becomes clear (Fig. 6b,c), characterized by a strong 114 to 128 kyr period (Fig. 7a). This amplitude modulation is interpreted as the influence of the short-eccentricity cycle. Analogous to the MS data, the constructed microfacies time-series (Fig. 6) is used instead of the distance-series to reenact spectral analysis on the "La Couvinoise" section as a whole. The resulting spectral plots (Fig. 7b)

CPD
7, 1427–1455, 2011

exhibit several significant spectral peaks that can be related to precession. Both the BT and the Walsh spectrum display a spectral peak at frequency 0.055 kyr^{-1} (18.3 kyr period). The BT spectrum shows an additional peak around 0.064 kyr^{-1} (15.6 kyr period), while the Walsh spectrum shows a second precession-related peak around 0.07 kyr^{-1} (14.3 kyr period). In the frequency range where half-precessional cycles are expected, i.e. between 0.10 and 0.14 kyr^{-1} (between 7 and 10 kyr periodicity), the BT and Walsh spectrum suggest 3 or 4 spectral peaks. Although not very extensive, these peaks seem to confirm the presence of an important half-precessional cycle. On Fig. 6a, the stratigraphic positions where half-precessional cycles are well developed in the microfacies curve are indicated by triangles.

Obviously, the amplitude modulation for both MS and microfacies must exhibit a similar pattern throughout the section to justify the interpretation of these modulations as eccentricity-forced. Therefore, the MS precessional cycles and their amplitude envelope (Fig. 6d) are plotted next to the microfacies precessional cycles and their amplitude envelope (Fig. 6b,c). The comparison of the two amplitude envelopes shows that they indeed show a similar development throughout the section and gives rise to the delineation of five full short-eccentricity cycles. The period of these eccentricity cycles between 92 and 131 kyr is in close agreement to the theoretical periods of short-eccentricity (i.e. 95 and 125 kyr).

So far, the amplitude modulation of the precession signal by eccentricity is seen as a confirmation of the astronomical interpretation. However, it is equally crucial to test the robustness of the amplitude modulation itself. In order to do so, following procedure was carried out: the magnetic susceptibility time-series consists of 338 points (Fig. 8a). The time-series was divided into 16 intervals of 20 points and an interval of 18 points. Of each interval, the maximal and minimal MS values were removed. In other words, 17 times 2 MS measurements were taken out of the time-series. The result is a time series with 304 points (i.e. 10 % less than the original time-series; Fig. 8b). This process, in which 17 times 2 points are deleted, was repeated to obtain a time-series with 270 points (i.e. 20 % less than the original time-series; Fig. 8c). In an analogous way,

CPD
7, 1427–1455, 2011

time-series consisting of 236 points (i.e. 30 % less than the original time-series; Fig. 8d) and 204 points (i.e. 40 % less than the original time-series; Fig. 8e) were created. The elimination of extreme points from the time-series only influences the amplitude modulation to a limited extent, and thus shows that the amplitude modulation is not the result of a few extreme MS values, but of a true amplitude modulation by eccentricity.

When the precessional variations in microfacies and MS are compared, it is clear that in the lower part of the section, these variations are in antiphase with each other (Fig. 9). In this part of the section, more proximal microfacies correspond to MS minima. To the contrary, in the upper part of the section, the precessional variations in the microfacies curve are in phase with precessional variations in the MS curve and thus proximal microfacies correspond to MS maxima (Fig. 9). This observation can be explained by the evolution of mean MS values on relative proximity transects (Fig. 9c; da Silva et al., 2009). In the lower part of the section, deposition occurred in an open marine environment. In such a setting, a shift to a more proximal environment is characterized by a higher carbonate productivity (diluting the MS signal) and water agitation (preventing the deposition of magnetic minerals). Conversely, in the upper part of the section, deposition occurred in a fore-reef environment. Here, shifts to a more proximal environment usually encompass the occurrence of peloidal(-crinoidal) pack- and grainstones. These microfacies, which are indicative for a more restricted environment, are characterized by a higher MS compared to the more distal fore-reef microfacies (Fig. 9c, da Silva et al., 2009).

4.2 Palaeoclimatological interpretation

The cycles driven by the astronomical parameters cannot be used as a geological metronome without an understanding of the way astronomical cycles influence the ferromagnetic minerals delivery processes towards the basin. The precessional forced MS variations in the “La Couvinoise” section are interpreted as the expression of variations in monsoon-circulation intensity. Here, we hypothesize how the

CPD
7, 1427–1455, 2011

monsoon-circulation, rainfall intensity and the continental detrital sediment flux depend on precession.

In Fig. 10, the monsoonal circulation on the east Euramerican continent is schematically illustrated and is based on the understanding of present monsoonal circulation. During Southern Hemispheric (SH) summer, a strong low-pressure cell develops above the Euramerican continent, allowing the Intertropical Convergence Zone (ITCZ) to cross the continent. Under such a configuration, the eastern part of the continent is dominated by a northeastern wind flow. During SH winter, the ITCZ zone is positioned in the Northern Hemisphere and the eastern part of the continent is dominated by the southeasterly trade winds.

Strong paleoclimate evidence from Africa, Australia, the Mediterranean and the Indian Ocean shows that today's monsoonal circulation is intensely controlled by precession (Clemens et al., 1991, 2010; Demenocal et al., 1993; Beaufort et al., 2010; Dickson et al., 2010; Ziegler et al., 2010). Most likely, similar mechanisms are responsible for the precessional cycles found in the studied "La Couvinoise" section. Therefore, we hypothesize that during a precession maximum, the Earth is situated near the perihelion (close to the sun) during austral summer solstice. This astronomical configuration causes a significant increase in the amount of insolation that reaches the southern subtropics during SH summer. The additional heat results in an intensified rising of warm air from the surface of the Euramerican continent. Consequently, a significantly deeper low-pressure cell develops above the continent pushing the ITCZ southwards compared to a "normal" Southern Hemispheric Summer. Consequently, the transequatorial pressure gradient between the continental low-pressure cell and the subtropical high-pressure cell in the north increases and causes an intensified monsoonal circulation. In other words, the intensified zonal pressure gradient during a precession maximum enhances wind velocity and enables an increased moisture transport towards the continent, leading to enhanced precipitation. More precipitation leads to increased runoff that in turn leads to an increased flux of detrital material from the continent to the marine system and consequently, to a maximum in magnetic susceptibility. Therefore,

CPD
7, 1427–1455, 2011

precessional forcing of the amount of precipitation appears as an important forcing factor in the subtropical climate during the Devonian.

However, the MS stratigraphy of the "La Couvinoise" section also revealed cyclicity at the frequency of half a precession cycle (~9.8 kyr). Berger et al. (2006) demonstrated the presence of an 11-kyr period in modern equatorial insolation. This sub-Milanković period, which is a harmonic of precession, is claimed to be found in paleoclimate archives of modern monsoonal systems (Hagelberg et al., 1994; Trauth et al., 2003; Turney et al., 2004; Sun and Huang, 2006; Verschuren et al., 2009). Several mechanisms were suggested to explain how the 11-kyr astronomical cycle is transferred to climate: an amplified response of tropical precipitation and temperature to changes in maximum summer insolation in both hemispheres (Hagelberg et al., 1994), atmospheric and oceanic teleconnections (Turney et al., 2004) low-latitude insolation forcing of monsoon-intensity (Short et al., 1991; Sun and Huang, 2006; Verschuren et al., 2009). Moreover, a coupled atmosphere/ocean/vegetation model demonstrated variations at periods of about 10 kyr in the monsoonal runoff, caused by the dynamic response of vegetation to precessional forcing (Tuenter et al., 2007). For the observed half-precession cyclicity in the "La Couvinoise" section, all above explanations have possibly contributed to the development of the half-precessional cycles in het MS record of the "La Couvinoise" section. More detailed climate study, involving climate modeling, will be needed to fully understand the relationship between the half-precession period in equatorial insolation and its consequences in tropical and monsoonal climates. However, the explicit identification of half-precessional cycles in the Middle-Devonian "La Couvinoise" climate record confirms the conclusion of Sun and Huang (2006) that climate systems with a more intense monsoonal circulation demonstrate an enhanced response to variations in low-latitude insolation, characterized by a half-precessional periodicity.

CPD
7, 1427–1455, 2011

5 Conclusions

Time series analyses of a high-resolution magnetic susceptibility signal from the Uppermost Eifelian and Lower Givetian of Southern Belgian indicates that astronomical forcing affects detrital input into the Rhenohercynian Basin. During the Uppermost Eifelian and Lower Givetian, the studied "La Couvinoise" magnetic susceptibility signal exhibits the direct influence of a 9.8 kyr half-precessional cycle and an 18 kyr-precessional cycle. Obliquity and eccentricity do not seem to strongly influence the MS signal, at least in a direct way. However, the amplitude-envelope of the precessional signal in MS and microfacies clearly demonstrates a ~100-kyr and/or ~405-kyr variation that can be attributed to short- and long-eccentricity, respectively. These results make us conclude that the climatically driven mechanisms, responsible for the input of detrital material in the Rheic Ocean, are precession-dominated. It is hypothesized that precession influences the transequatorial pressure gradient and its consequent monsoonal dynamics. The recognition of a half-precessional cycle suggests the importance of low-latitude insolation forcing of intense monsoonal systems.

Acknowledgement. This study was made possible thanks to a Ph.D. fellowship of the Research Foundation – Flanders (FWO). A. C. da Silva acknowledges the FRS-FNRS (Fond National de la Recherche Scientifique) for a post doctoral position. Ph. Claeys thanks the VUB research fund for support.

References

Beauchamp, K. G.: Applications of Walsh and Related Functions, with an Introduction to Sequency Theory, Academic Press, New York, 1975.

Beaufort, L., van der Kaars, S., Bassinot, F. C., and Moron, V.: Past dynamics of the Australian monsoon: precession, phase and links to the global monsoon concept, Clim. Past, 6, 695–706, doi:10.5194/cp-6-695-2010, 2010.

Berger, A., Loutre, M. F., and Laskar, J.: Stability of the astronomical frequencies over the Earth's history for Paleoclimate studies, Science, 255, 560–565, 1992.

CPD

7, 1427–1455, 2011

Berger, A., Loutre, M. F., and Mélice, J. L.: Equatorial insolation: from precession harmonics to eccentricity frequencies, Clim. Past, 2, 131–136, doi:10.5194/cp-2-131-2006, 2006.
Berner, R. A.: GEOCARBSULF: a combined model for Phanerozoic atmospheric O_2 and CO_2, Geochim. Cosmochim. Acta, 70, 5653–5664, doi:10.1016/j.gca.2005.11.032, 2006.
Bloomfield, P.: Fourier Analysis of Time Series: An Introduction, Wiley, New York, 288 pp., 2004.
Boulvain, F., Mabille, C., Poulain, G., and da Silva, A. C.: A magnetic susceptibility curve for the Devonian Limestone from Belgium, Geol. Belgica, 13, 113–117, 2010.
Bultynck, P., Dreesen, R., Groessens, E., Struwe, W., Weddige, K., Werner, R., and Ziegler, W.: Field Trip A, 1st International Senckenberg Conference and 5th European Conodont Symposium (ECOS V), Contributions I, Guide to Field Trips, Courier Forschungsinsitut Senckenberg, Frankfurt, Germany, 1988.
Cecil, C. B.: Paleoclimate controls on stratigraphic repetition of chemical and siliciclastic rocks, Geology, 18, 533–536, 1990.
Clemens, S., Prell, W., Murray, D., Shimmield, G., and Weedon, G.: Forcing mechanisms of the Indian Ocean monsoon, Nature, 353, 720–725, 1991.
Clemens, S. C., Prell, W. L., and Sun, Y. B.: Orbital-scale timing and mechanisms driving Late Pleistocene Indo-Asian summer monsoons: reinterpreting cave speleothem δO^{-18}, Paleoceanography, 25, PA4207, doi:10.1029/2010pa001926, 2010.
Copper, P.: Silurian and Devonian reefs: 80 million years of global greenhouse between two ice ages, Soc. Econ. Paleontol. Mineralog. Spec. Publ., 72, 181–238, 2002.
da Silva, A. C., Mabille, C., and Boulvain, F.: Influence of sedimentary setting on the use of magnetic susceptibility: examples from the Devonian of Belgium, Sedimentology, 56, 1292–1306, 2009.
Dekker, S. C., Rietkerk, M., and Bierkens, M. F. P.: Coupling microscale vegetation-soil water and macroscale vegetation-precipitation feedbacks in semiarid ecosystems, Global Change Biol., 13, 671–678, 2007.
Demenocal, P. B., Ruddiman, W. F., and Pokras, E. M.: Influences of high-latitude and low-latitude processes on African terrestrial climate – Pleistocene Eolian records from Equatorial Atlantic-Ocean drilling program site-663, Paleoceanography, 8, 209–242, 1993.
Dickson, A. J., Leng, M. J., Maslin, M. A., and Rohl, U.: Oceanic, atmospheric and ice-sheet forcing of South East Atlantic Ocean productivity and South African monsoon intensity during MIS-12 to 10, Quaternary Sci. Rev., 29, 3936–3947, doi:10.1016/j.quascirev.2010.09.014,

CPD
7, 1427–1455, 2011

2010.
Ellwood, B. B., Crick, R. E., El Hassani, A., Benoist, S. L., and Young, R. H.: Magnetosusceptibility event and cyclostratigraphy (MSEC) in marine rocks and the question of detrital input versus carbonate productivity, Geology, 28, 1135–1138, 2000.
Flohn, H., Kapala, A., Knoche, H. R., and Maechel, H.: Water vapour as an amplifier of the greenhouse effect, Meteorol. Z., 1, 122–138, 1992.
Ghil, M., Allen, M. R., Dettinger, M. D., Ide, K., Kondrashov, D., Mann, M. E., Robertson, A. W., Saunders, A., Tian, Y., Varadi, F., and Yiou, P.: Advanced spectral methods for climatic time series, Rev. Geophys., 40, 1–41, doi:10.1029/2000RG000092, 2002.
Hagelberg, T. K., Bond, G., and Demenocal, P.: Milankovitch band forcing of sub-Milankovitch climate variability during the Pleistocene, Paleoceanography, 9, 545–558, 1994.
Hays, J., Imbrie, J., and Shackleton, N.: Variations in the Earth's Orbit: pacemaker of the Ice Ages, Science, 194, 1121–1132, 1976.
Hladil, J., Gersl, M., Strnad, L., Frana, J., Langrova, A., and Spisiak, J.: Stratigraphic variation of complex impurities in platform limestones and possible significance of atmospheric dust: a study with emphasis on gamma-ray spectrometry and magnetic susceptibility outcrop logging (Eifelian-Frasnian, Moravia, Czech Republic), Int. J. Earth Sci., 95, 703–723, 2006.
Kaufmann, B.: Calibrating the Devonian Time Scale – a synthesis of U-Pb ID-TIMS ages and relative, time-linear conodont stratigraphy, Earth-Sci. Rev., 76, 175–190, doi:10.1016/j.earscirev.2006.01.001, 2006.
Kutzbach, J. E.: Monsoon climate of the early holocene – climate experiment with the Earths orbital parameters for 9000 years ago, Science, 214, 59–61, 1981.
Kutzbach, J. E. and Liu, Z.: Response of the African monsoon to orbital forcing and ocean feedbacks in the Middle Holocene, Science, 278, 440–443, 1997.
Kutzbach, J. E., Bonan, G., Foley, J., and Harrison, S. P.: Vegetation and soil feedbacks on the response of the African monsoon to orbital forcing in the early to middle Holocene, Nature, 384, 623–626, 1996.
Mabille, C. and Boulvain, F.: Sedimentology and MS of the Upper Eifelian – Lower Givetian (Middle Devonian) in Southwestern Belgium: insights into carbonate platform initiation, in: Palaeozoic Reefs and Bioaccumulations: Climatic and Evolutionary Controls, edited by: Alvaro, J. J., Aretz, M., Boulvain, F., Munnecke, A., Vachard, D., and Vennin, E., Geological Society Special Publications, London, 109–124, 2007.

CPD
7, 1427–1455, 2011

Muller, R. A. and MacDonald, G. J.: Ice ages and astronomical causes, Data, Spectral Analysis and Mechanisms, Springer, London, 318 pp., 2000.
Niedzwiedzki, G., Szrek, P., Narkiewicz, K., Narkiewicz, M., and Ahlberg, P. E.: Tetrapod trackways from the early Middle Devonian period of Poland, Nature, 463, 43–48, 2010.
Paillard, D., Labeyrie, L., and Yiou, P.: Macintosh program performs time-series analysis, Eos Trans. AGU, 77, 379, 1996.
Proakis, J. G. and Menolakis, D. G.: Digital Signal Processing, Principles, Algorithms and Applications, Prentice Hall, London, 1996.
Rind, D., Chiou, E. W., Chu, W., Larsen, J., Oltmans, S., Lerner, J., Mccormick, M. P., and Mcmaster, L.: Positive Water-Vapor Feedback in Climate Models Confirmed by Satellite Data, Nature, 349, 500–503, 1991.
Riquier, L., Averbuch, O., Devleeschouwer, X., and Tribovillard, N.: Diagenetic versus detrital origin of the magnetic susceptiblity variations in some carbonate Frasnian-Famennian boundary sections from Northern Africa and Western Europe: implications for paleoenvironmental reconstructions, Int. J. Earth Sci., 99, 57–73, 2010.
Short, D. A., Mengel, J. G., Crowley, T. J., Hyde, W. T., and North, G. R.: Filtering of Milankovitch cycles by Earths geography, Quaternary Res., 35, 157–173, 1991.
Streel, M., Caputo, M. V., Loboziak, S., and Melo, J. H. G.: Late Frasnian-Famennian climates based on palynomorph analyses and the question of the Late Devonian glaciations, Earth-Sci. Rev., 52, 121–173, 2000.
Sun, J. M. and Huang, X. G.: Half-precessional cycles recorded in Chinese loess: response to low-latitude insolation forcing during the Last Interglaciation, Quaternary Sci. Rev., 25, 1065–1072, doi:10.1016/j.quascirev.2005.08.004, 2006.
Thomson, D. J.: Spectrum estimation and harmonic-analysis, Proc. IEEE, 70, 1055–1096, 1982.
Trauth, M. H., Deino, A. L., Bergner, A. G. N., and Strecker, M. R.: East African climate change and orbital forcing during the last 175 kyr BP, Earth Planet. Sc. Lett., 206, 297–313, doi:10.1016/S0012-821x(02)01105-6, 2003.
Tuenter, E., Weber, S. L., Hilgen, F. J., and Lourens, L. J.: The response of the African summer monsoon to remote and local forcing due to precession and obliquity, Global Planet. Change, 36, 219–235, 2003.

CPD
7, 1427–1455, 2011

Tuenter, E., Weber, S. L., Hilgen, F. J., and Lourens, L. J.: Simulating sub-Milankovitch climate variations associated with vegetation dynamics, Clim. Past, 3, 169–180, doi:10.5194/cp-3-169-2007, 2007.

Turney, C. S. M., Kershaw, A. P., Clemens, S. C., Branch, N., Moss, P. T., and Fifield, L. K.: Millennial and orbital variations of El Nino/Southern Oscillation and high-latitude climate in the last glacial period, Nature, 428, 306–310, doi:10.1038/Nature02386, 2004.

Verschuren, D., Damste, J. S. S., Moernaut, J., Kristen, I., Blaauw, M., Fagot, M., and Haug, G. H.: Half-precessional dynamics of monsoon rainfall near the East African Equator, Nature, 462, 637–641, doi:10.1038/Nature08520, 2009.

Weddige, K.: Die Conodonten der Eifel-Stufe im Typusgebiet und in benachbarten Faziesgebieten, Senckenbergiana Lethaea, 58, 271–419, 1977.

Weedon, G. P.: The detection and illustration of regular sedimentary cycles using Walsh power spectra and filtering, with examples from the Lias of Switzerland, J. Geol. Soc. London, 146, 133–144, 1989.

Weedon, G. P.: Time-Series Analysis and Cyclostratigraphy: Examining Stratigraphic Records of Environmental Cycles, Cambridge University Press, Cambridge, UK, New York, xiii, 259 pp., 2003.

Westphal, H., Bohm, F., and Bornholdt, S.: Orbital frequencies in the carbonate sedimentary record: distorted by diagenesis?, Facies, 50, 3–11, doi:10.1007/s10347-004-0005-x, 2004.

Ziegler, M., Tuenter, E., and Lourens, L. J.: The precession phase of the boreal summer monsoon as viewed from the Eastern Mediterranean (ODP Site 968), Quaternary Sci. Rev., 29, 1481–1490, doi:10.1016/j.quascirev.2010.03.011, 2010.

CPD
7, 1427–1455, 2011

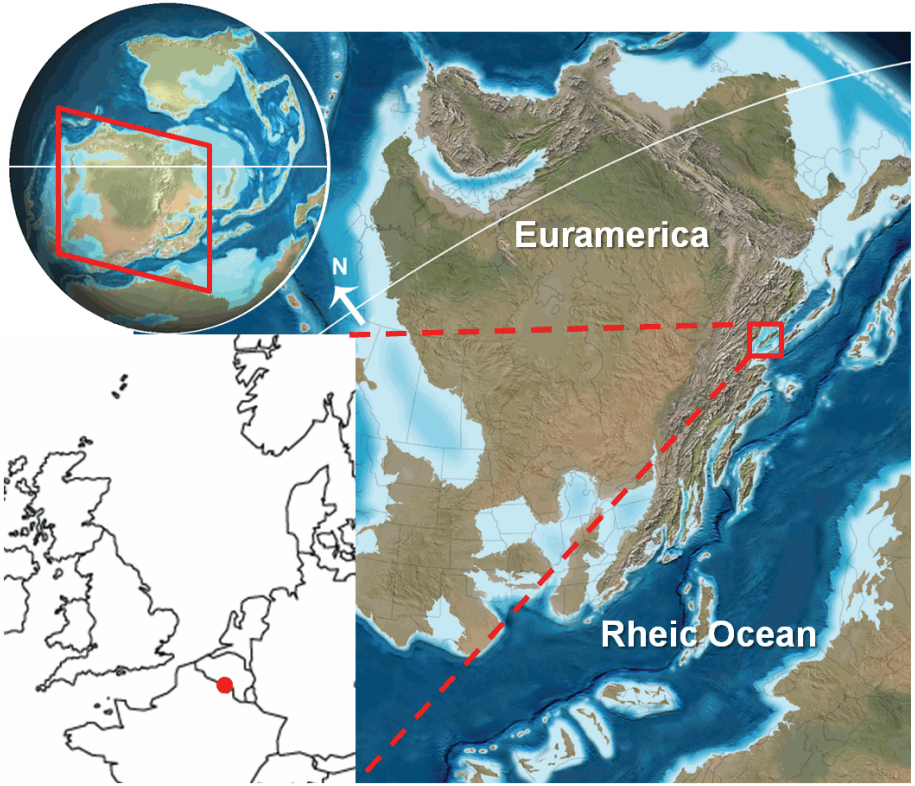

Fig. 1. Mid-Devonian paleogeography (after Ron Blakey, Norhtern Arizona University Geology) and situation of “La Couvinoise” section.

CPD
7, 1427–1455, 2011

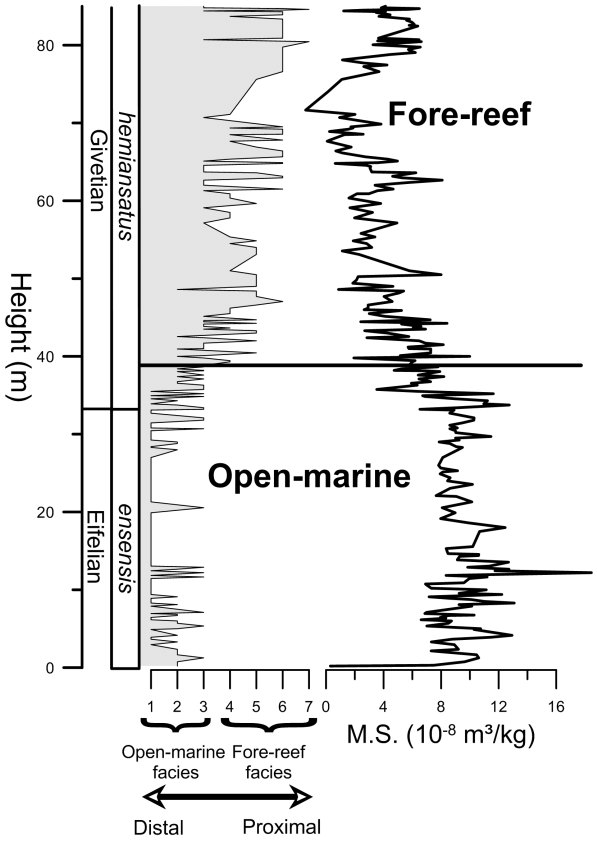

Fig. 2. The "La Couvinoise" section: magnetic susceptibility and facies belts (modified after Boulvain et al., 2010). Key to facies numbers: 1 = Argillaceous mudstone; 2 = Argillaceous bioclastic wackestone; 3 = Brachiopods-crinoids argillaceous packstones; 4 = Floatstones and rudstones with reefal debris; 5 = Stromatoporoids bindstones; 6 = Peloidal packstones-grainstones; 7 = Peloidal-crinoidal grainstones.

CPD
7, 1427–1455, 2011

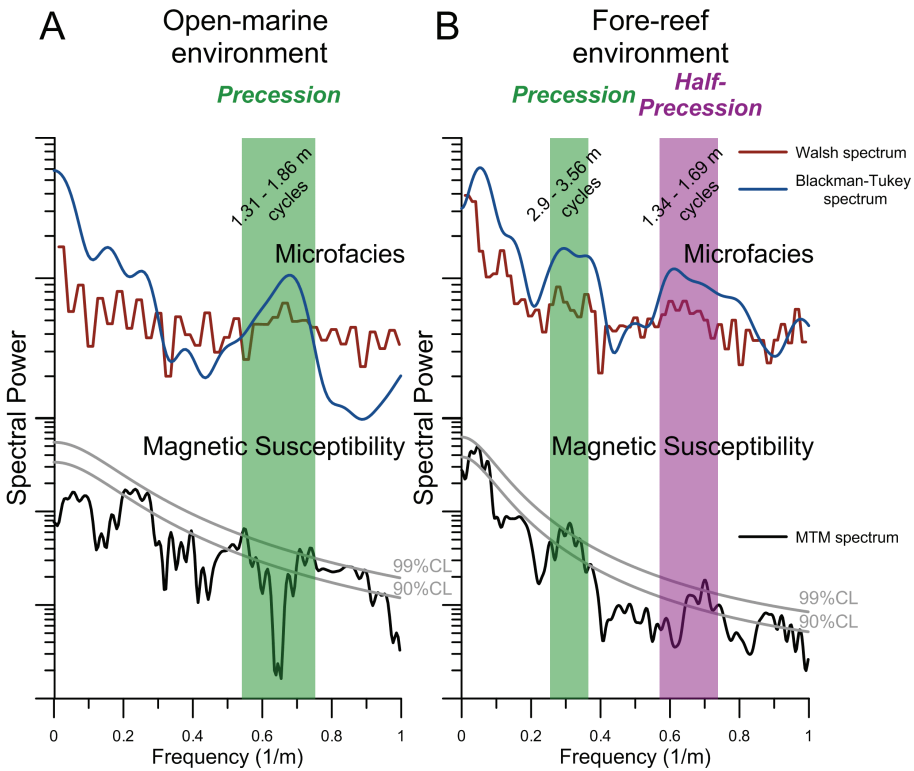

Fig. 3. Spectral analyses on the different depositional environments of the "La Couvinoise" section separately. **(A)** Spectral analyses on the microfacies series and magnetic susceptibility series of the lower part of the section (open marine environment). **(B)** Spectral analyses on the microfacies series and magnetic susceptibility series of the upper part of the section (fore-reef environment). CL = confidence limit.

CPD
7, 1427–1455, 2011

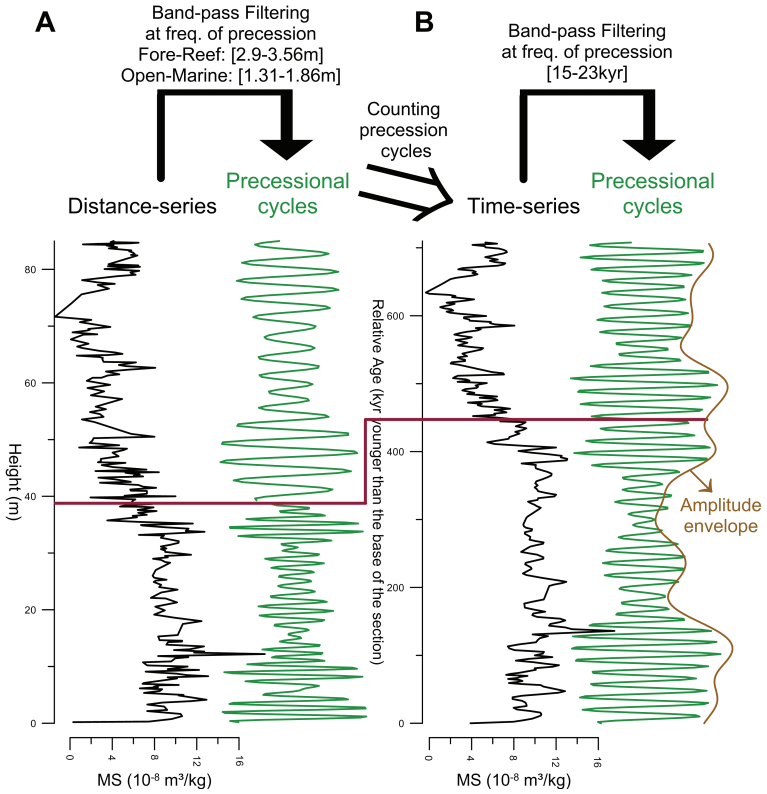

Fig. 4. From distance-series to time-series. **(A)** Magnetic susceptibility series of the "La Couvinoise" section plotted against a distance-axis (black) and band-pass filtered magnetic susceptibility signal at the frequencies of precession (green, band-pass filtered between 1.31–186 m in the lower part and between 2.9–3.56 m in the upper part of the section). **(B)** Magnetic susceptibility series of the "La Couvinoise" section plotted against a time-axis (black) and band-pass filtered magnetic susceptibility signal at the frequency of precession (band-pass filtered between 15 and 23 kyr; green) + amplitude envelope of the precessional signal (brown).

CPD
7, 1427–1455, 2011

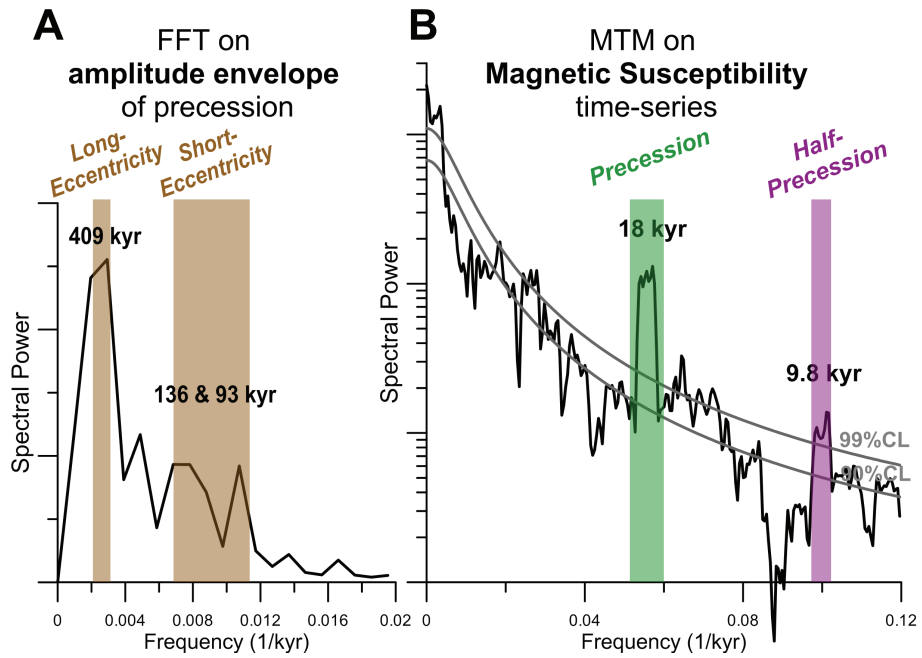

Fig. 5. Spectral analyses on the MS series of the "La Couvinoise" section as a whole. **(A)** Fast Fourier Transform (FFT) periodogram of the amplitude envelope of the precessional signal. A linear "spectral power" axis is chosen to give an immediate sense of how much of the variance comes from each cycle. **(B)** Multitaper method (MTM) power spectrum of the "La Couvinoise" MS data as a time-series. A logarithmic "spectral power" axis is chosen to make the statistical significance of peaks evident, particularly for small high-frequency peaks. CL = confidence limit.

CPD
7, 1427–1455, 2011

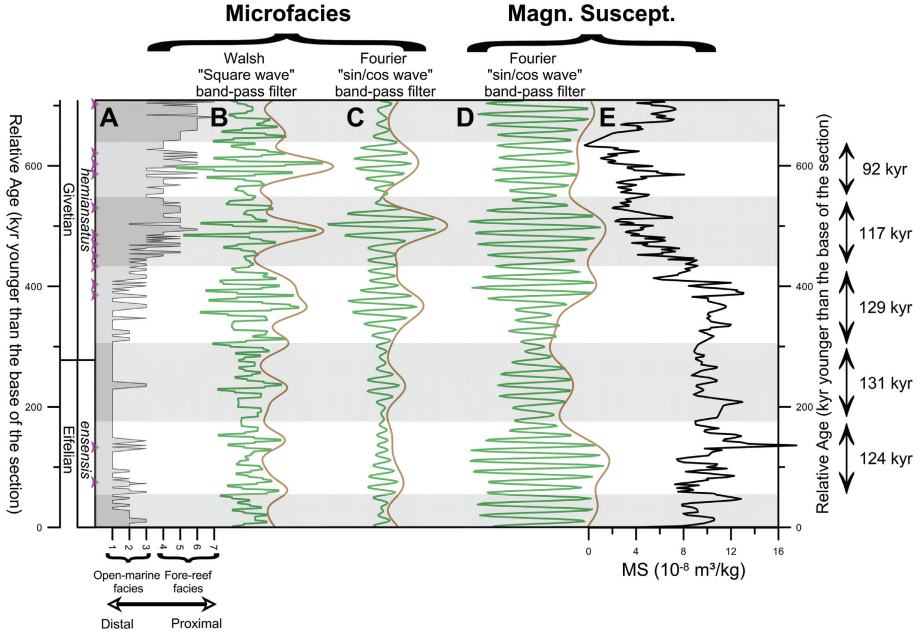

Fig. 6. **(A)** Microfacies series of the "La Couvinoise" section plotted against a time-axis. **(B)** Band-pass filtered microfacies signal at the frequency of precession (filtered between 15 and 23 kyr; green) based on the Walsh Transform + amplitude envelope (brown). **(C)** Band-pass filtered microfacies signal at the frequency of precession (15–23 kyr; green) based on the Fourier Transform + amplitude envelope (brown). **(D)** Band-pass filtered MS signal at the frequency of precession (15–23 kyr; green) based on the Fourier Transform + amplitude envelope (brown). **(E)** MS signal of the "La Couvinoise" section plotted against a time-axis. Triangles indicate those precessional cycles within which the half-precessional cycles are well-developed.

CPD
7, 1427–1455, 2011

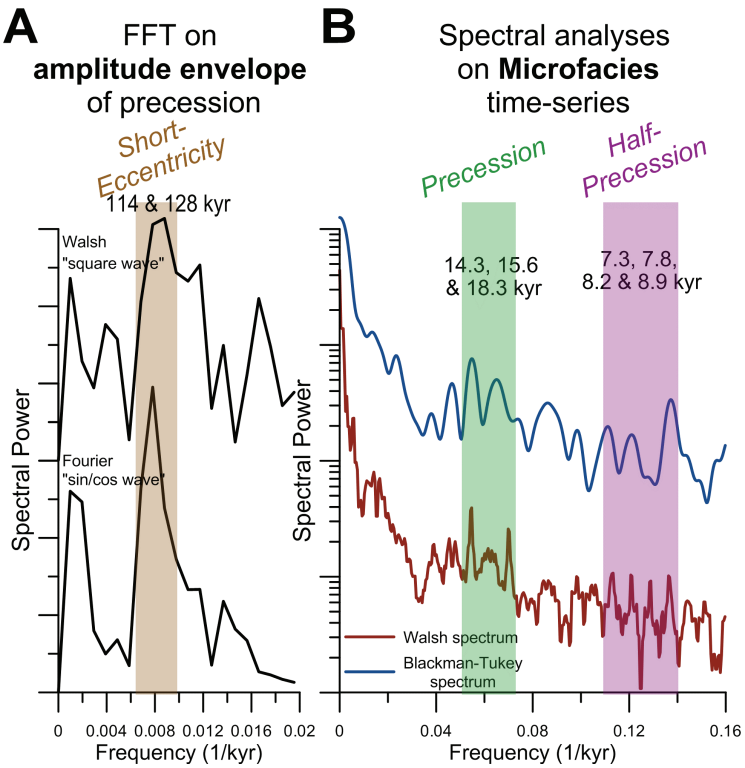

Fig. 7. Spectral analyses on the microfacies series of the "La Couvinoise" section as a whole. **(A)** FFT periodogram of the amplitude envelope of the precessional signal. Upper: based on Walsh Transform (Fig. 6b); Lower: based on Fourier Transform (Fig. 6c). A linear "spectral power" axis is chosen to give an immediate sense of how much of the variance comes from each cycle. **(B)** MTM power spectrum of the "La Couvinoise" microfacies curve as a time-series. A logarithmic "spectral power" axis is chosen to make the statistical significance of peaks evident, particularly for small high-frequency peaks. CL = Confidence Limit.

CPD
7, 1427–1455, 2011

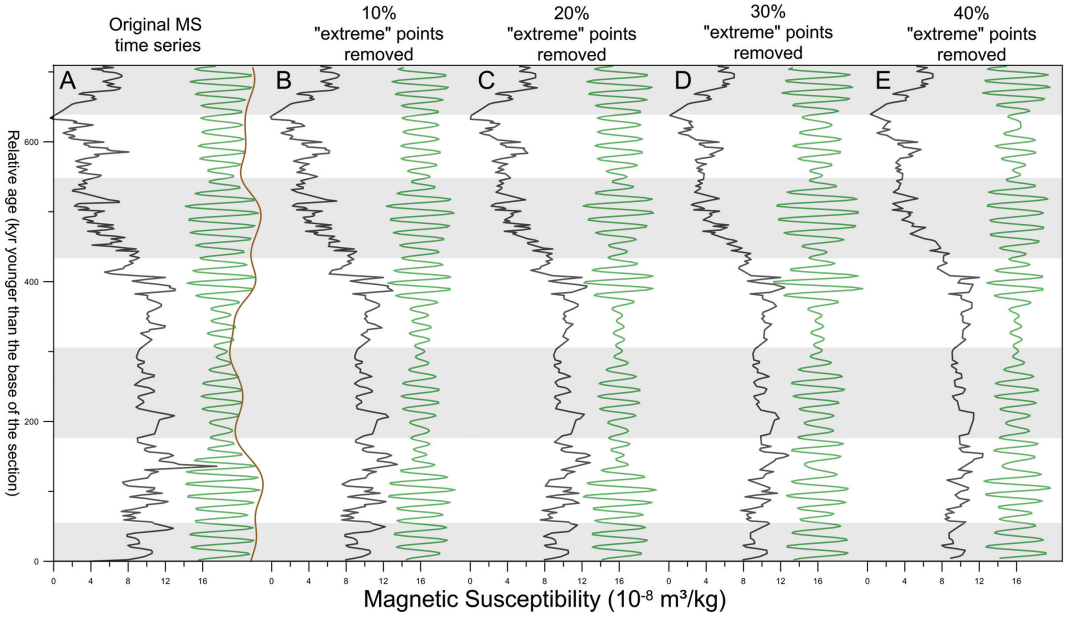

Fig. 8. Robustness-test of the amplitude modulation of the precessional signal in the MS time-series. **(A)** Origninal MS time-series (black), its precessional signal (green) and the amplitude envelope of the precessional singal (brown). **(B–E)** MS time-series of which the 10 % – 20 % – 30 % – 40 % most extreme MS values are removed (black) and its precessional signal (green).

CPD
7, 1427–1455, 2011

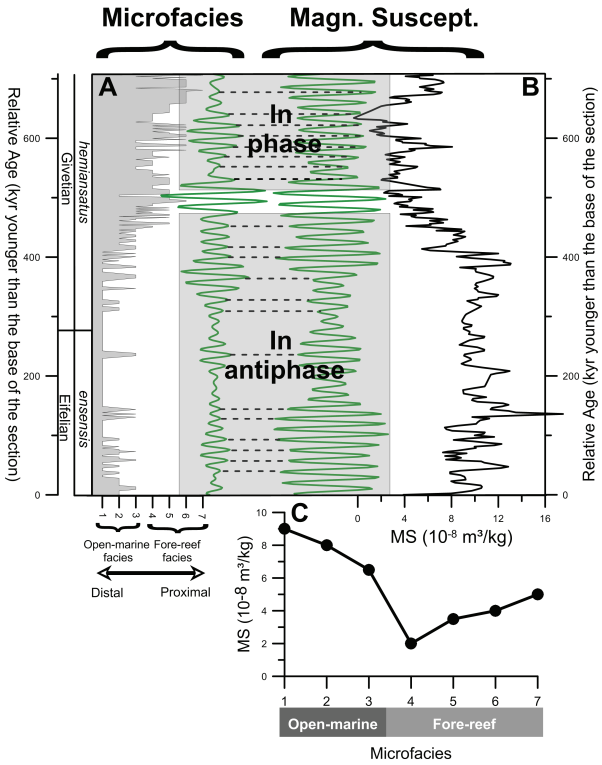

Fig. 9. Precessional microfacies variation vs. precessional magnetic susceptibility variation. **(A)** Microfacies curve plotted against a time-axis and band-pass filtered microfacies curve at the frequency of precession (between 15 and 23 kyr; left). **(B)** Magnetic susceptiblity series plotted against a time-axis and band-pass filtered MS series at the frequency of precession (between 15 and 23 kyr; right). **(C)** Evolution of mean MS values on a relative proximity transect (after da Silva et al., 2009). The reversal of the slope of the MS evolution on a relative proximity transect explains why precession-scale variations of microfacies and MS are in antiphase in the lower part of the section and in phase in the upper part of the section.

CPD
7, 1427–1455, 2011

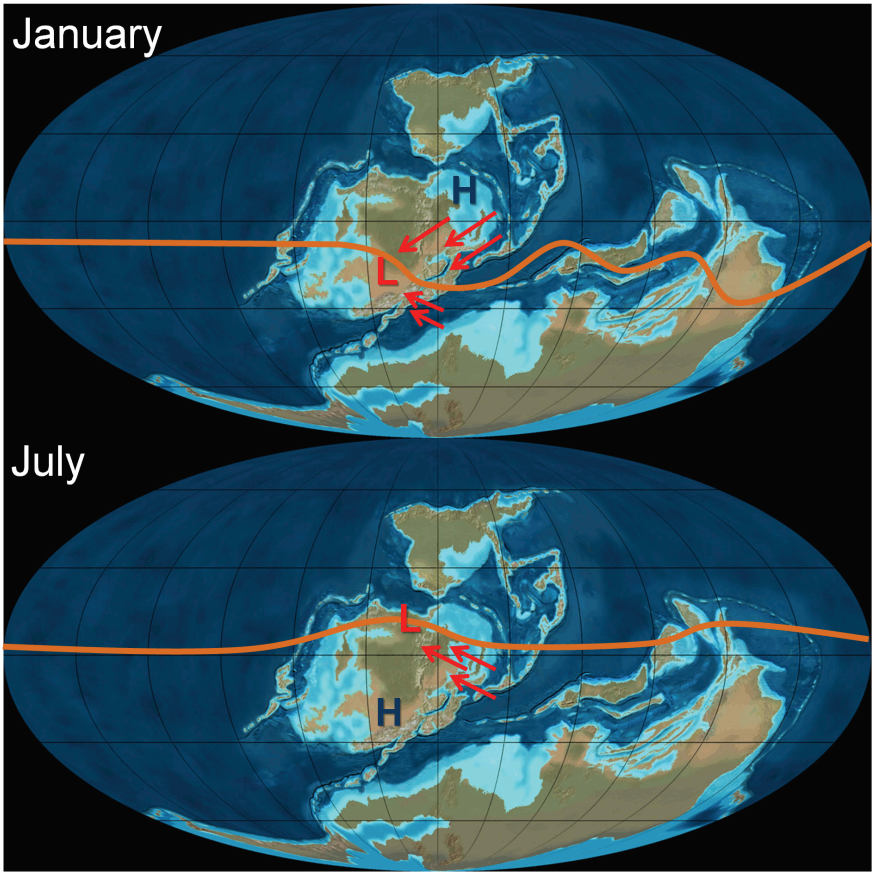

Fig. 10. Monsoon-like circulation in Eastern Euramerica during the Mid-Devonian (Paleogeographic map from Ron Blakey, Northern Arizona University Geology). Intertropical Convergence Zone (ITCZ) in orange. Important trade winds are indicated by red arrows. L: Low pressure cell. H: High pressure cell.

CPD
7, 1427–1455, 2011